

# Improvement of critical current densities in $\text{SmBa}_2\text{Cu}_3\text{O}_y$ films with $\text{BaHfO}_3$ nano-rods using low temperature growth technique

Shun Miura<sup>1</sup>, Yutaka Yoshida<sup>1</sup>, Yusuke Ichino<sup>1</sup>, Ataru Ichinose<sup>2</sup>,  
Kaname Matsumoto<sup>3</sup> and Satoshi Awaji<sup>4</sup>

<sup>1</sup>Department of Energy Engineering and Science, Nagoya University, Furo-cho, Chikikusa-ku, Nagoya 464-8603, Japan

<sup>2</sup>Electric Power Engineering Research Laboratory, Central Research Institute of Electric Power Industry, 2-6-1 Nagasaka, Yokosuka, Kanagawa 240-0196, Japan

<sup>3</sup>Department of Materials Science and Engineering, Kyushu Institute of Technology, 1-1 Sensui-cho, Tobata-ku, Kitakyushu 804-8550, Japan

<sup>4</sup>Institute for Materials Research, Tohoku University, Katahira 2-1-1, Aoba-ku, Sendai 980-8577, Japan

E-mail: miura-syun12@ees.nagoya-u.ac.jp

**Abstract.** We studied growth substrate temperature dependent morphologies of  $\text{BaHfO}_3$  (BHO) nano-rods for  $\text{SmBa}_2\text{Cu}_3\text{O}_y$  (SmBCO) films with BHO fabricated by pulsed laser deposition (PLD) method. The morphology of BHO nano-rods within the SmBCO matrix could be controlled by changing substrate temperatures adopting a Low Temperature Growth (LTG) technique. Using the LTG technique, we could fabricate SmBCO films showed *c*-axis orientation even at low substrate temperature during deposition without a degradation of superconducting properties, which is one of the most advantages of the LTG technique. In this study, we found an optimal morphology of the BHO nano-rods and the morphology was fine, straight and various growth directions. The BHO nano-rods were more effective to improve the  $J_c$  in a magnetic field than other morphologies of the BHO nano-rods.

## 1. Introduction

$\text{REBa}_2\text{Cu}_3\text{O}_y$  (RE: Y and rare-earth elements, REBCO) superconductors are very promising materials, because they have high critical temperatures ( $T_c$ s). Research and development of electrical power applications, such as cables, superconducting magnetic energy storage and magnetic resonance imaging, using the REBCO films have been actively carried out [1]. For the applications, it is necessary to improve the critical current density ( $J_c$ ) of REBCO films in magnetic fields. In order to improve the  $J_c$  of REBCO films in magnetic fields, it is effectively to introduce a non-superconducting second phase into a REBCO matrix. Size of the non-superconducting second phase is ideally hoped to be similar to vortex core (~10 nm, for *ab* plane at 77 K).  $\text{BMO}_3$  (M: Zr, Sn and Hf, BMO) is very famous vortex pinning centres for *c*-axis of REBCO matrix. The BMO formed “nano-rods” in REBCO matrix which fabricated by vapour phase deposition method such as pulsed laser deposition (PLD) and chemical vapour deposition (CVD). The BMO nano-rods become correlated pinning centres for *c*-axis of a REBCO matrix. Furthermore, morphologies of the BMO nano-rods could be controlled by deposition condition such as substrate temperatures, laser repetition rates and BMO content during



deposition [2-5]. In order to control flux pinning properties of BMO nano-rods in REBCO matrix, it is necessary to control the morphologies of the BMO nano-rods. In this paper, we focus on growth substrate temperatures during deposition. The morphology of BHO nano-rods within the SmBCO matrix was controlled by changing substrate temperatures adopting a Low Temperature Growth (LTG) technique. Using the LTG technique, we could fabricate SmBCO films which showed *c*-axis orientation even at low substrate temperature without a degradation of superconducting properties. In this work, we carried out to control morphologies of BHO nano-rods and compared the flux pinning properties of the BHO nano-rods in SmBCO films.

## 2. Experimental details

All films in this study were deposited on a LaAlO<sub>3</sub> (100) single-crystal substrates by PLD method using a KrF ( $\lambda = 248$  nm) excimer laser at a repetition rate of 10 Hz. The laser energy density and distance between substrate and targets were 2.0 J/cm<sup>2</sup> and 45 mm, respectively. All the films were fabricated by LTG technique. The LTG technique consists of the following two steps. Firstly, a thin SmBCO seed layer was deposited at the relatively high substrate temperature, in order to form a purely *c*-axis oriented SmBCO film on a substrate. Secondly, a SmBCO upper layer was homoepitaxially grown on the seed layer. A SmBCO seed layer was deposited at 850 °C with a thickness of about 50 nm on the substrate, and then an upper layer of BHO doped SmBCO was grown at 700 ~ 840 °C with a thickness of about 500 nm on the seed layer. Then, we define substrate temperatures of upper layer as  $T_s^{\text{upper}}$ . We applied an alternating targets (ALT) technique to introduce BHO into the SmBCO upper layer. The ALT technique is a way to obtain films with a designed composition by exchanging two different targets alternately. In this study, we used a pure SmBCO target and a pure BHO target to deposit the BHO doped SmBCO films via the ALT technique. The number of total irradiation times with pulse laser of upper layer of the SmBCO target and the BHO target are 24000 (= 30 pulses  $\times$  800) and 1600 (= 2 pulses  $\times$  800), respectively. O<sub>2</sub> partial pressure during the deposition was 400 mTorr.

The crystalline orientation of the films was evaluated by X-ray diffraction (XRD) analysis and microstructure of the films was observed by high-resolution transmission electron microscope (TEM). The BHO contents were measured by inductively coupled plasma-atomic emission spectroscopy (ICP-AES). In this paper, BHO contents of the SmBCO films were 2.7 vol.%. The resistivity and critical current at various magnetic fields were measured by standard four-probe method with a physical properties measurement system (PPMS : Quantum Design). A  $T_c$  was defined from a temperature dependence of resistivity by using the resistivity criterion of 0.1  $\mu\Omega\text{cm}$  and the probe current was fixed to about 25 A/cm<sup>2</sup>. The  $J_c$  was evaluated from current vs. voltage curves with electric field criterion of

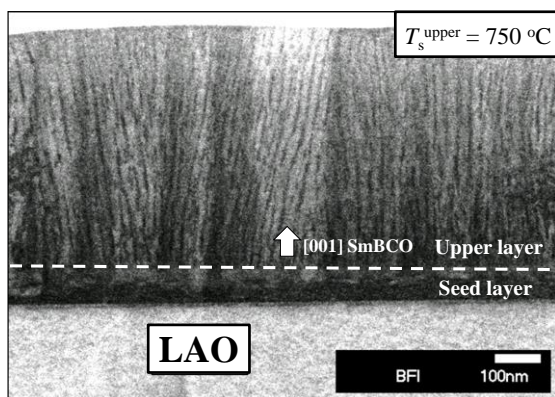


Figure 1 A cross-sectional TEM image of 2.7 vol.% BaHfO<sub>3</sub>-doped SmBa<sub>2</sub>Cu<sub>3</sub>O<sub>y</sub> film fabricated at  $T_s^{\text{upper}}$  of 750 °C.

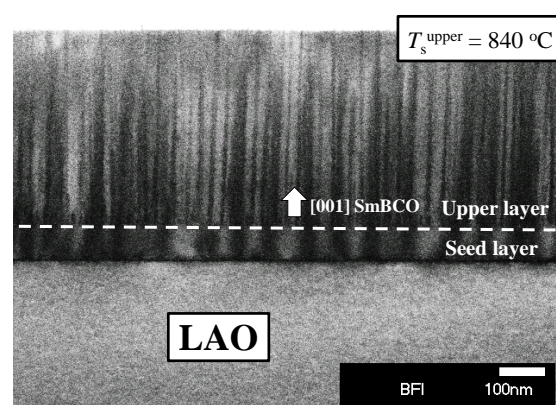


Figure 2 A cross-sectional TEM image of 2.7 vol.% BaHfO<sub>3</sub>-doped SmBa<sub>2</sub>Cu<sub>3</sub>O<sub>y</sub> film fabricated at  $T_s^{\text{upper}}$  of 840 °C.

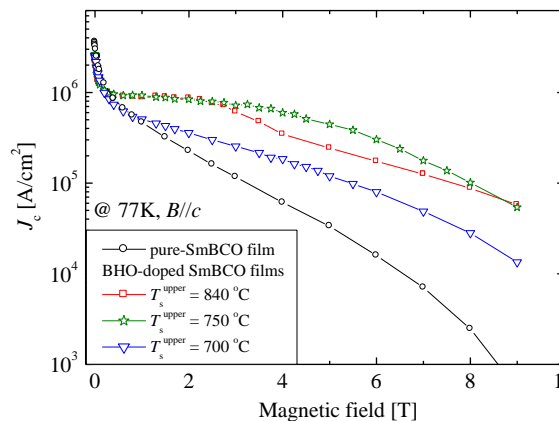


Figure 3 Magnetic field dependence of  $J_c$ s of  $B//c$  for BHO-doped SmBCO films and a pure-SmBCO film.

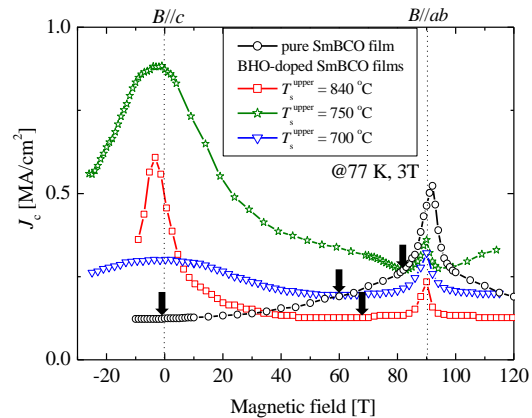


Figure 4 Field angular dependence of  $J_c$ s for the BHO-doped SmBCO films and a pure-SmBCO film.

1  $\mu$ V/cm at 77 K. Thicknesses of the films were measured by the TEM and ICP-AES. From the measurements, thicknesses of the films were about 500 nm.

### 3. Results and discussion

Firstly, in order to investigate morphologies of BHO nano-rods within a SmBCO film fabricated by the LTG technique at various substrate temperatures, microstructures in the LTG-SmBCO + BHO films were measured by TEM images. Figure 1 shows a cross-sectional TEM image of the BHO-doped LTG-SmBCO film fabricated at relatively low substrate temperature,  $T_s^{\text{upper}} = 750$  °C. The BHO formed fine and long nano-rods with the diameter and the number density of about 5.7 nm and 2300 / $\mu\text{m}^2$ , respectively. Then the matching field ( $B_\phi$ ) calculated by the number density was 4.7 T. Another important feature is that some BHO nanorods inclined for  $c$ -axis of the SmBCO. On the other hand, morphologies of BHO nano-rods within a SmBCO film fabricated at relatively high substrate temperature ( $T_s^{\text{upper}} = 840$  °C) were different from that of the  $T_s^{\text{upper}} = 750$  °C sample. Figure 2 shows a cross-sectional TEM image of the BHO-doped LTG-SmBCO film fabricated at  $T_s^{\text{upper}} = 840$  °C. The BHO formed fat nano-rods and grown straightly along with the  $c$ -axis of SmBCO. The diameter and the number of the BHO nano-rods were about 8.5 nm and 1440 / $\mu\text{m}^2$ , respectively. Then the matching field ( $B_\phi$ ) calculated by the number density was 3.0 T. Based on these, we successfully controlled morphologies of BHO nano-rods in SmBCO films by changing substrate temperature.

We discuss flux pinning properties of the BHO nano-rods in SmBCO films fabricated at  $T_s^{\text{upper}} = 700, 750$  and 840 °C. We show magnetic field dependence of  $J_c$ s at 77 K of  $B//c$  for the BHO-doped SmBCO films and a pure-SmBCO film in Figure 3. The  $J_c$  of all the BHO-doped films in high magnetic field were higher than that of the pure-SmBCO film.  $T_s^{\text{upper}} = 750$  °C and 840 °C samples showed plateau regions in the  $J_c$ - $B$  curves. In addition, the ending points of these plateau regions are about  $B_\phi$ . In the plateau regions, fluxes motion in the films was reduced because BHO nano-rods are occupied by magnetic fluxes. Thus, in this magnetic field range,  $J_c$  is not affected to applied magnetic field. On the other hand, there was no plateau region on the  $J_c$ - $B$  curve of  $T_s^{\text{upper}} = 700$  °C sample. It was likely to be due to becoming the BHO to particles or very short nano-rods.

We show the applied field angular dependences of  $J_c$  at 77 K in 3 T for the BHO-doped SmBCO films fabricated at various  $T_s^{\text{upper}}$  and the pure-SmBCO film in Figure 4. We can confirm the  $J_c$  peak for  $B//c$  of  $T_s^{\text{upper}} = 750$  °C sample was the highest in this study. Furthermore, the  $J_c$  value in applied magnetic field angular of a wide range (0 ~ 80 °) was higher than that of the pure-SmBCO film. Then, we focus on the detailed shapes of the  $J_c$  peaks for  $B//c$ , the widths of the peaks became broader with  $T_s^{\text{upper}}$  decreasing. The  $T_s^{\text{upper}}$ -dependent change could occur as the result of a change in BHO

morphologies with  $T_s^{\text{upper}}$ . In other word, the vortex pinning by inclined the BHO nano-rods could lead to a broader  $J_c$  peak for  $B//c$ . In Figure 4, the minimum  $J_c$  values ( $J_c^{\text{min}}$ ) are indicated by arrows. The  $J_c^{\text{min}}$  of  $T_s^{\text{upper}} = 750$  °C sample was higher than other samples, the  $J_c^{\text{min}}$  value was  $0.27 \text{ MA/cm}^2$  (77 K, 3 T). It was confirmed that various growth directions of the BHO nano-rods was effective to improve the  $J_c^{\text{min}}$ . Superior properties were also found in the angular dependence of  $J_c$  of the  $T_s^{\text{upper}} = 750$  °C sample compared with the other samples remarkably in this study. Because, maybe the BHO nano-rods became high number density and grew to the various directions.

#### 4. Conclusion

The relationships between morphologies of BHO nano-rods and flux pinning properties were clarified in the SmBCO films with BHO nano-rods. We succeeded in controlling the morphologies of the BHO nano-rods by growth substrate temperatures. It could be confirmed that BHO nano-rods of  $T_s^{\text{upper}} = 750$  °C sample were inclined for  $c$ -axis of SmBCO matrix. In addition, these BHO nano-rods formed fireworks structures. In the future, understanding the mechanism of the formation of the fireworks structures will help us to control morphologies of BHO more effectively. In this study, we found an optimal morphology of BHO nano-rods which was fine, straight and various growth directions. The BHO nano-rods were more effective to improve the  $J_c^{\text{min}}$  than other morphologies of BHO nano-rods.

#### Acknowledgment

This work was partly supported by Grants-in-Aid for Scientific Research (19676005, 23226014 and 25289358) from the Japan Society for the Promotion of Science (JSPS).

#### References

- [1] Shiohara Y, Fujiwara N, Hayashi H, Nagaya S, Izumi T and Yoshizumi M 2009 *Physica C* **469** 863
- [2] Ozaki T, Yoshida Y, Ichino Y, Takai Y, Ichinose A, Matsumoto K, Horii S, Mukaida M and Takano Y 2010 *J. Appl. Phys.* **108** 093905
- [3] Haruta M, Ichinose A, Fujita N, Saura K, Maeda T and Horii S 2013 *IEEE Trans. Appl. Supercond.* **23** 8000904
- [4] Ichinose A, Naoe K, Horide T, Matsumoto K, Kita R, Mukaida M, Yoshida Y and Horii S 2007 *Supercond. Sci. Technol.* **20** 1144
- [5] B Maiorov, S A Baily, H Zhou, O Ugurlu, J A Kennison, P C Dowden, T G Holesinger, S R Foltyn and L Civale 2009 *Nature Materials* **8** 398
- [6] A Ichinose, P Mele, K Matsumoto, H Kai, M Takamura, K Yamada, M Mukaida, S Horii, S Funaki, Y Ichino, Y Yoshida and R Kita 2009 *Phys. C* **469** 1374